Waste Management 174 (2024) 351–361

Contents lists available at ScienceDirect

Waste Management

journal homepage: www.elsevier.com/locate/wasman

Research Paper

Hydraulic conductivity of geosynthetic clay liners to trona ash leachate: Effects of mass per unit area, bundles of fiber existence, and preydration conditions

Asena İ. Demir Sürer [a], Tuğçe Özdamar Kul [b], A. Hakan Ören [b,*]

[a] Dokuz Eylul University, Graduate School of Natural and Applied Sciences, 35390 Buca-Izmir, Turkiye
[b] Dokuz Eylul University, Dept. of Civil Engineering, 35390 Buca-Izmir, Turkiye

ARTICLE INFO

Keywords:
Hydraulic conductivity
geosynthetic clay liner (GCL)
Trona ash leachate
Mass per unit area
Prehydration

ABSTRACT

The barrier performance of geosynthetic clay liners (GCLs) to coal combustion products (CCPs) is of primary importance. One of the CCPs leachates that has a damaging effect on hydraulic conductivity is trona ash leachate (TAL). In this study, the hydraulic conductivity of sodium GCL (Na-GCL) to TAL was investigated in terms of mass per unit area (MPUA). The hydraulic conductivity of GCLs to TAL was 2.6×10^{-6} and 7.6×10^{-7} m/s when the MPUA was 3.0 kg/m^2 (M_{b3}) and 4.0 kg/m^2 (M_{b4}), respectively. Dye tests conducted on these GCLs showed that flow preferentially occurred through bundles of fibers existing in the GCLs. In contrast, increasing the MPUA to 5.0 kg/m^2 (M_{b5}) led to a decrease in the hydraulic conductivity (i.e. 4.1×10^{-11} m/s). Additional tests were performed on fiber-free GCLs to determine the role of fiber bundles. Regardless of MPUA, the fiber-free GCLs had low hydraulic conductivity (6.7×10^{-11} m/s). Prehydrating M_{b3} and M_{b4} with deionized water (DIW) before permeation with TAL also decreased the hydraulic conductivity. The hydraulic conductivities of prehydrated M_{b3} and M_{b4} were 1.6×10^{-10} and 4.8×10^{-11}, respectively. Chemical analyses showed that the cation exchange reaction had a negligible influence on the hydraulic conductivity. Because TAL was a potential source of Na^+ throughout the tests.

1. Introduction

Coal combustion products (CCPs) are residues of coal combustion obtained from coal-fired power plants. CCPs include fly ash, bottom ash, flue gas desulfurization materials, and other by-products of coal combustion (Benson et al., 2018a; Chen et al., 2019, 2018; Tan et al., 2022; Zainab et al., 2021). Relative to the source of coal, CCPs potentially contain toxic substances such as arsenic, cadmium, and lead, which threaten the environment and human health (Environmental Protection Agency (EPA), 2015; Jones et al., 2012; Ruhl et al., 2012; Wang et al., 2021). CCPs release various major and trace cations and anions when in contact with water. As a result, wastewater can leak and contaminate groundwater in CCP waste disposal areas. Prevention of contamination is important in terms of environmental pollution and human health (Benson et al., 2018b; Chen et al., 2019, 2018; Environmental Protection Agency (EPA), 2015; Yang et al., 2018).

Storing the aqueous form of CCP waste in ponds is the most preferred method (i.e., surface impoundment, mine and quarry fill, and ocean disposal) worldwide (Sönmez and Işık, 2020; Zhang, 2014). In Türkiye, the Turkish Statistical Institute announced in News Bulletin 37,198 that 24.4 million tons of CCPs were released from thermal power plants in 2020 (Türkiye İstatistik Kurumu (TÜİK), 2021). According to the United States Environmental Protection Agency (USEPA) report published in the Federal Register on April 17, 2015 (Environmental Protection Agency (EPA), 2015), over 470 coal-fired electric utilities burned almost 800 million tons of coal in 2012, producing roughly 110 million tons of CCPs in the United States. Approximately 40 % of the generated CCPs were beneficially used, while the remaining 60 % were disposed of in surface impoundments and landfills. To prevent potential contamination of groundwater, the USEPA requires the CCP disposal facilities to have a composite liner consisting of at least 0.75-mm geomembrane (GM) overlying a 0.6-m deep compacted clay liner (CCL). In addition, the Federal Register rules require that the hydraulic conductivity of CCLs should be less than 1.0×10^{-9} m/s. The regulation allows the use of alternative materials such as geosynthetic clay liners (GCLs) if they provide the hydraulic conductivity requirements in lieu of CCLs.

* Corresponding author.
E-mail addresses: asenairem.demir@ogr.deu.edu.tr (A.İ. Demir Sürer), tugce.ozdamar@deu.edu.tr (T. Özdamar Kul), ali.oren@deu.edu.tr (A. Hakan Ören).

https://doi.org/10.1016/j.wasman.2023.11.033
Received 3 April 2023; Received in revised form 7 November 2023; Accepted 25 November 2023
Available online 13 December 2023

GCLs are composite materials that consist of a thin layer of sodium bentonite (Na-B) sandwiched between two geotextiles and have low hydraulic conductivity to water ($<2.0 \times 10^{-11}$ m/s) (Bouazza, 2002a; Bradshaw et al., 2013; De Camillis et al., 2016; Kolstad et al., 2004; Petrov et al., 1997; Ruhl and Daniel, 1997; Scalia et al., 2014; Setz et al., 2017; Shackelford et al., 2000). GCLs have been used as hydraulic barriers in lagoons, landfill liner systems, and mine waste containment to limit the flow of leachate through the environment. The limitation of flow is interpreted in terms of the hydraulic conductivity of GCL to site-specific solutions (Jo et al., 2005; Petrov et al., 1997).

The bentonite portion of the material governs the hydraulic conductivity of GCLs, which is naturally enriched by sodium or modified by polymers. Bentonite is primarily composed of montmorillonite minerals that have high swelling potential and hence low hydraulic conductivity ($<2.0 \times 10^{-11}$ m/s). Osmotic swelling of bentonite particles is responsible for the low permeability, resulting in tortuous flow paths for mobile water (Akin and Chen, 2017; Benson et al., 2010; Bradshaw et al., 2013; Chen et al., 2019; Di Emidio et al., 2015; Guyonnet et al., 2009; Jo et al., 2005, 2001; Kolstad et al., 2004; Mazzieri et al., 2013; Ören and Akar, 2017; Scalia et al., 2014; Shackelford et al., 2000; Wang et al., 2019). The hydraulic performance of GCLs has been investigated using inorganic industrial solutions such as mine tailings and wastewater. Several researchers have reported that aggressive leachates with high ionic strength and a predominance of multivalent cations suppress the swelling of montmorillonite, resulting in large pores between particles and high hydraulic conductivity for GCLs (Chen et al., 2019, 2018; Katsumi et al., 2008; Mazzieri et al., 2013; Mazzieri and Emidio, 2015; Naka et al., 2019; Ören et al., 2018; Setz et al., 2017; Wang et al., 2019; Zainab et al., 2021; Zainab and Tian, 2020).

The studies reported so far have investigated the effect of polymer loading on the barrier performance of GCLs to CCPs leachates and compared the results with those of conventional Na-GCLs (Chen et al., 2019, 2018; Wireko et al., 2022; Zainab et al., 2021). In these studies, the hydraulic conductivity of Na-GCLs to CCPs leachates was generally greater than that of polymer-rich GCLs (P-GCLs). However, the polymerization process causes polymer GCLs (P-GCLs) to be more expensive than conventional Na-GCLs. Moreover, Na-GCLs can be found in most parts of the world, which makes Na-GCL a more cost-effective material than P-GCL. Although the barrier performance of Na-GCL to CCP has been reported in detail (Chen et al., 2019, 2018; Zainab et al., 2021), none of these studies reported the results in terms of bentonite mass per unit area (MPUA). Therefore, investigating and discussing the hydraulic performance of Na-GCL to TAL in terms of MPUA may provide some insights for engineers who work with GCLs.

MPUA generally varies within a GCL roll. Bentonite in GCL can migrate when installed on slopes or in sumps in landfills. Similarly, irregularity in the subgrade conditions and the existence of wrinkles on the geomembrane overlying the GCL result in non-uniform stress conditions, leading to bentonite migration in the GCL (Fox et al., 1998; Stark et al., 2004). Recent studies have shown the significance of bentonite mass per unit area (MPUA) on the hydraulic conductivity of GCLs (Ören et al., 2022; Rowe and Hamdan, 2021a; Salemi et al., 2018; Von Maubeuge and Ehrenberg, 2014). An increase in the MPUA led to a slight decrease in the hydraulic conductivity of GCLs when DIW was the permeant (Ören et al., 2022; Von Maubeuge and Ehrenberg, 2014). However, the hydraulic conductivity of GCLs to inorganic solutions is generally unpredictable because the existence of bundles of fibers on GCLs plays an important role when MPUA is low (Rowe et al., 2017; Rowe and Hamdan, 2021).

As can be seen from the literature, MPUA has negligible influence on the hydraulic conductivity of GCLs to water. However, it is unknown whether MPUA influences hydraulic conductivity when the permeant is other than water. To fill the gap in the literature, the barrier performance of Na-GCL to TAL was investigated at various MPUAs (between 3.0 and 5.0 kg/m^2). The existence of bundles of fibers on GCLs and hydration conditions before permeation were considered as factors affecting hydraulic conductivity. The findings were discussed with respect to the cation exchange mechanism, which plays a significant role in transmitting the flow through the bundle of fibers. The main motivation of this work was to provide a new insight to engineers regarding the barrier performance of Na-GCL in terms of MPUA. Na-GCL was used in this study to show that polymer loading is not the only way of decreasing the hydraulic conductivity.

2. Background: Hydraulic conductivity of GCLs to trona ash leachate (TAL) and leachates comparable to TAL

Depending on the ionic strength, the CCPs leachates may alter the swelling potential of GCLs, and hence hydraulic conductivity. Therefore, when GCLs are considered for use in CCP disposal facilities, their chemical compatibility with CCPs leachates should be considered. Among CCPs leachates, trona ash leachate (TAL) is more aggressive than others because it has high values of ionic strength ($I = \frac{1}{2}\sum c_i z_i^2$, where c_i and z_i are the molar concentration and the valence of i^{th} ion, respectively) and relative abundance of monovalent to divalent cations ($RMD = \frac{M_M}{\sqrt{M_D}}$, where M_M and M_D are the total molarity of monovalent and divalent cations, respectively) (Chen et al., 2019, 2018).

Chen et al. (2018) examined the hydraulic conductivity of two Na-GCLs to TAL. Both GCLs had sand-sized granules and denoted as CS and GS. GS contains finer granules than CS. MPUA of both GCLs was 3.76 ± 0.12 kg/m^2. Hydraulic conductivity tests were conducted on non-prehydrated and subgrade hydrated GCLs at effective stresses ranging from 20 to 450 kPa. The hydraulic conductivities of non-prehydrated CS and GS-GCLs to TAL was 1.2×10^{-6} and 5.4×10^{-8} m/s, respectively, when the effective stress was 20 kPa. Increasing the effective stress to 450 kPa decreased the hydraulic conductivity to 1.1×10^{-9} and 5.3×10^{-11} m/s for both GCLs, respectively. Subgrade hydrated GCLs had lower hydraulic conductivity than non-prehydrated GCLs (direct permeation of TAL), although the effect of subgrade hydration on hydraulic conductivity was modest. The hydraulic conductivities of subgrade-hydrated CS and GS-GCLs to TAL was 2.6×10^{-6} and 1.5×10^{-8} m/s at 20 kPa and was 5.0×10^{-10} and 1.8×10^{-11} m/s at 450 kPa effective stresses, respectively. Prehydration of CS and GS-GCLs with DIW before TAL decreased the hydraulic conductivity to 7.0×10^{-10} and 6.4×10^{-11} m/s when the effective stress was 20 kPa.

Chen et al. (2019) reported the influence of polymer loading on the hydraulic conductivity of bentonite polymer composite (BPC) GCLs to TAL. The MPUA of Na-GCLs was within the range of 3.6 – 3.7 kg/m^2. The hydraulic conductivity of BPC GCLs with low polymer loading was similar to that of conventional Na-GCLs. The hydraulic conductivities of non-prehydrated and subgrade hydrated BPC GCL with 1.2 % polymer loading was 5.0×10^{-7} m/s and 6.8×10^{-7} m/s, respectively. Further increase in the polymer loading reduced the hydraulic conductivity of BPC-GCLs to TAL. Above 1.2 % polymer loading (up to 10.9 %), the hydraulic conductivities of BPC-GCLs varied between 1.0×10^{-10} m/s and 3.3×10^{-12} m/s depending on the granule size of bentonite and prehydration conditions.

Zainab et al. (2021) performed hydraulic conductivity tests on seven GCLs using synthetic CCP leachates. One GCL was conventional sodium bentonite (Na–B) and the other six were bentonite-polymer (B–P) mixtures with polymer loadings ranging from 0.5 % to 12.7 %. The MPUA of Na-GCL was 4.0 kg/m^2, whereas that of B-P GCLs was between 4.8 and 6.8 kg/m^2. One of the CCPs leachates had a relatively comparable ionic strength (3179 mM) and RMD (32.02 M$^{1/2}$) to that of TAL (the denotation of the leachate was HI). Unless a polymer loading of 12.7 % (B-P-12.7) was used, Na-GCL and all B–P GCLs had high hydraulic conductivity to HI ($>3.0 \times 10^{-8}$ m/s). When the polymer loading was increased to 12.7 %, the hydraulic conductivity decreased to 8.6×10^{-12} m/s.

Wireko et al. (2022) reported the hydraulic performance of GCLs to incineration ash leachates. Two types of conventional Na-GCLs and six bentonite polymer composite GCLs with polymer loadings ranging from

0.5 % to 5.5 % were used. The MPUA of conventional GCLs was ~ 4.2 kg/m^2 and that of B-P GCLs was within the range of 4.1 – 5.5 kg/m^2. Among the incineration ash leachates, the ionic strength and RMD of the co-disposal (CD-AVG and CD-MAX) and ash-monofil (AM-AVG and AM-MAX) leachates were comparable to those of TAL. The hydraulic conductivity of both conventional GCLs had high hydraulic conductivity to those leachates (>3.0 × 10^{-7} m/s). The hydraulic conductivity slightly decreased to the range of 7.4 × 10^{-7} – 2.6 × 10^{-9} m/s with the same leachates when the B-P GCLs contained 5.5 % crosslinked polymers.

3. Materials and methods

3.1. Geosynthetic clay liner

Needle-punched Na-GCL obtained from a local manufacturer was used in this study. The liquid and plastic limits of sodium bentonite were determined in accordance with ASTM D4318–17 (2017) and were 231 % and 61 %, respectively. The swell index of bentonite was 22.5 mL/2g (ASTM D5890-19, 2019). The mass per unit area (MPUA) of the GCL was determined following ASTM D5993–99, (2010), which ranged between 2.9 and 6.5 kg/m^2 throughout the roll. To investigate the influence of MPUA on hydraulic conductivity, GCLs with varying MPUA were cut into 100-mm-diameter pieces and stored in plastic bags. Among these samples, GCLs with MPUA of 3.0 ± 0.3, 4.0 ± 0.3, and 5.0 ± 0.3 kg/m^2 were selected and used in hydraulic conductivity tests. For simplicity, GCL samples with MPUA of 3.0 ± 0.3, 4.0 ± 0.3, and 5.0 ± 0.3 kg/m^2 are denoted as M_{b3}, M_{b4}, and M_{b5}, respectively. Some physical properties of Na-GCL are summarized in Table S1 of the SupplementaryMaterial.

3.2. Synthetic trona ash leachate

Trona Ash Leachate (TAL) was prepared in the laboratory as suggested by Benson et al. (2018a). For this purpose, reagent grade calcium sulfate ($CaSO_4$), sodium sulfate (Na_2SO_4), magnesium sulfate ($MgSO_4$), and potassium sulfate (K_2SO_4) were dissolved in deionized water (DIW). DIW was collected from the Milli-Q Gradient water purification system. Synthetic leachate was stored in 5-L plastic containers. The chemical composition of TAL is given in Table S2.

3.3. Preparation of Fiber-Free GCLs

The woven and non-woven geotextiles supplied by the GCL manufacturer were used during the preparation of fiber-free GCLs. Samples of 100-mm diameter were cut from each geotextile (Fig. S1a). Bentonite was extracted from the GCL roll and dried in an oven at 105 °C to determine the water content. To achieve the target MPUA, sufficient air-dried bentonite was weighed. A woven geotextile was placed on the base pedestal of the permeameter cell, and a thin wall of bentonite paste was built along the perimeter of the base pedestal to prevent bentonite loss from the GCL during pouring of bentonite and side wall leakage during permeation (Fig. S1b). Bentonite was poured over the woven geotextile, and the surface was flattened using a spatula (Fig. S1c). Finally, a non-wowen geotextile was placed over the bentonite, and the GCL was covered with a latex membrane. O-rings were placed on the top and bottom pedestals (Fig. S1d). More details regarding sample preparation

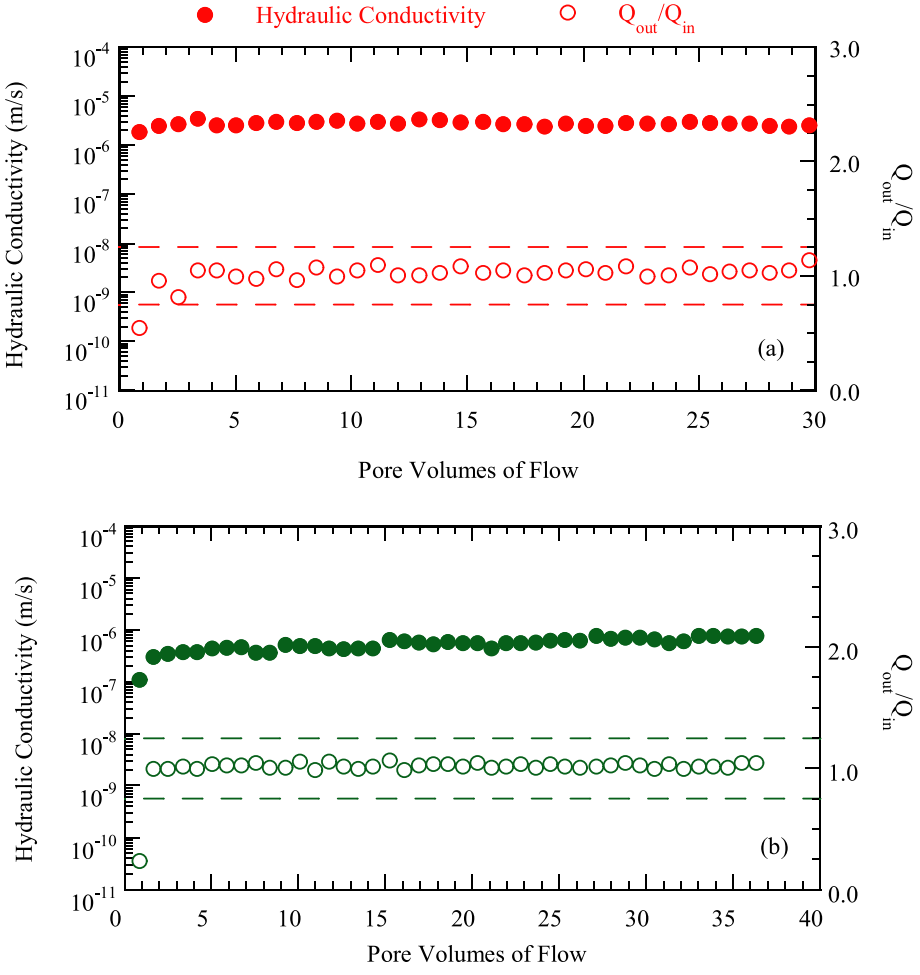

Fig. 1. Hydraulic conductivity of GCL as a function of PVF: a) Mass per unit area (MPUA) of 3.0 kg/m^2 (M_{b3}) and b) MPUA of 4.0 kg/m^2 (M_{b4}).

can be found in Demir Sürer (2023).

3.4. Swell index (SI) test

Bentonite taken from GCL was ground in a mortar and sieved through a No. 200 US standard sieve. The powdered bentonite was dried in an oven at 105 °C for 24 h before testing. DIW and TAL were used as the reagent water for the tests. The swell index of the GCL was determined according to ASTM D5890-19 (2019).

3.5. Hydraulic conductivity tests

Hydraulic conductivity tests were conducted using flexible wall permeameters and applying a falling head and constant tail water method as described in ASTM:D6766-14 (2014). GCL samples were cut in 100-mm diameter from the roll, and the mass of each sample was recorded. Then, GCL was placed between the top and base pedestals of the permeameters. Non-woven geotextiles with a 100-mm diameter were placed between the GCL and the pedestals (either top or bottom) to homogeneously distribute the inflow through the GCL and outflow from the GCL. To prevent sidewall leakage, the perimeter of the GCL was sealed with bentonite paste. The GCL was then covered with a latex membrane, and three O-rings were attached to the top and bottom pedestals to enhance sealing.

The barrier performance of a material is usually determined under low effective stress conditions during hydraulic conductivity tests. Because an increase in the effective stress decreases the hydraulic conductivity (Benson et al., 2018a; Liu et al., 2015; Wang et al., 2019). The hydraulic gradient applied during the tests should also simulate the field conditions. A high hydraulic gradient means that the water head over the barrier is high, which can facilitate the flow of water across the barrier material (Rowe et al., 2017). Since the thickness of GCLs is much lower than that of compacted clay liners (CCLs), the hydraulic gradient applied on GCLs is 10 times greater than that applied on CCLs (for example, 100 vs 10). To simulate the field conditions as much as possible, hydraulic conductivity tests were conducted under a cell pressure of 35 kPa and an average hydraulic gradient of 45.

For the non-prehydrated case, GCL was hydrated with TAL for 24 h by keeping the outflow valve closed and the inflow valve open. Generally, 48 h of hydration duration is applied for the non-prehydration case (Chen et al., 2018; Jo et al., 2005, 2004, 2001; Lee and Shackelford, 2005); however, Polat (2022) showed that the GCL water content reached equilibrium after 24 h of hydration, which is close to the water content of GCL hydrated over compacted silty sand for 30 days. Thus, 24 h of hydration duration with TAL was applied before permeation. After 24 h, permeation was initiated with TAL by opening the outflow valve. In the prehydrated case, the GCL was initially permeated with DIW by passing 2 pore volumes of flow (PVF) across the GCL. The GCL can be prehydrated with DIW under zero hydraulic gradient conditions, such as by opening the influent valve and closing the outflow valve for several days (Shackelford et al., 2000; Benson et al., 2010). Alternatively, prehydration can be applied by permeating the GCL with DIW for a while (several PVF) before permeating the GCL with the test liquid (Lee and Shackelford, 2005; Shackelford et al., 2000; Shackelford and Sample-Lord, 2014). PVF was calculated considering the initial condition of the GCL. Petrov et al. (1997) showed how to calculate PVF in a GCL. Once the prehydration stage was completed, the permeant solution was switched to the TAL. The program for the hydraulic conductivity test is summarized in Fig. S2. Tests were terminated when hydraulic and chemical equilibrium was established. To achieve hydraulic equilibrium, the outflow-to-inflow ratio should be within 1 ± 0.25. Chemical equilibrium was also established when the-effluent-to-influent ratio of pH, electrical conductivity (EC) and the concentrations of major bound cations (i.e., Na^+, K^+, Ca^{2+} and Mg^{2+}) and anion (SO_4^{2-}) were within ± 10 %.

3.6. Chemical analysis

Liquid samples were collected from the influent and effluent ends of the permeameter during the hydraulic conductivity test. The pH and EC of the influent and effluent samples were measured using Accumet XL50 bench-top meters. The probes were calibrated using the related buffer solutions before measurement. To determine the exchangeable ions released from the bentonite, cation and anion analyses were conducted on the influent and effluent samples using inductively coupled plasma optical emission spectrometry (ICP-OES).

The bound cations of GCLs were determined according to ASTM: D7503–18, (2020). Initially, 10 g of air-dried bentonite was sieved from the No. 10 standard sieve and then mixed with 40 mL of ammonium acetate (NH_4OAc) at a concentration of 1 M in a plastic bottle. The suspension was then shaken with an end-over-end shaker at 30 rpm for 5 min. The suspension was left for 24 h. After 24 h, the suspension was shaken again for 15 min at 30 rpm and filtered through Whatman No. 42 (2.5 μm) ashless filter paper using a Buchner funnel. Bentonite was washed with 30 mL of NH_4OAc solution 4 times by applying < 10 kPa vacuum pressure. At the end of washing, the filtrate was analyzed by ICP-OES to determine the major bound cations (i.e., Na^+, K^+, Ca^{2+} and Mg^{2+}).

4. Results and discussion

4.1. Influence of MPUA on hydraulic conductivity

The hydraulic conductivity of the GCLs was initially determined using DIW. Table 1 summarizes the hydraulic conductivities in terms of MPUA and test duration. The hydraulic conductivity of M_{b3}, M_{b4}, and M_{b5} to DIW was low and within the range of $4.6 \times 10^{-11} - 2.1 \times 10^{-11}$ m/s. The hydraulic conductivity of Na-GCL slightly decreased as the MPUA of GCL increased, which agrees with the findings of Ören et al. (2022) and Von Maubeuge and Ehrenberg (2014).

The hydraulic conductivity behaviors of M_{b3} and M_{b4} to TAL are shown in Fig. 1a-b. The hydraulic conductivities of M_{b3} and M_{b4} were high throughout the test duration and were finally around 2.6×10^{-6} m/s and 7.6×10^{-7}, respectively. To observe the flow paths occurring across the GCLs, the influent solutions were spiked with a pink rhodamine dye (5 mg/l). After the pink dye flowed through the GCLs, the tests were terminated, and pictures of M_{b3} and M_{b4} were taken with a camera (Fig. 2a and b). Woven geotextiles were removed from both GCLs after cutting the needle-punched fibers with a scalpel. Extra care was taken to not disturb the specimens. The traces of the flow paths on both GCLs, which are colored pink as can be seen in Fig. 2a-d. Fig. 2c-d, also show bundles of fibers and holes that are free of bundles. Some bundles of fibers were left on the woven geotextile, while cutting and holes were left behind when the geotextile was removed.

The existence of bundles of fibers caused the occurrence of flow paths across the GCLs (Fig. 2c-d). These bundles of fibers acted as flow channels, which conducted the flow easily. Although bentonite was mostly in a homogeneous form, remnant granules remained in both GCLs (Fig. 2c-d). Because the ionic strength of TAL is high (i.e., I = 1190 mM), the bentonite granules exhibited crystalline swelling rather than osmotic swelling. Indeed, the swell index of bentonite in TAL was 8.0 mL/2g. Hence, the pressure acting on the bundles of fibers by the bentonite granules was not sufficiently high to fully close the bundles of fiber-induced flow paths. Therefore, the hydraulic conductivity of M_{b3} and M_{b4} was quite high. Since the hydraulic conductivity of M_{b3} and M_{b4} was above the allowable limit (1.0×10^{-9} m/s), chemical analyses were not conducted on these GCLs.

Further increase in the bentonite mass in GCL (i.e. M_{b5}) showed different type of hydraulic behavior. Hydraulic conductivity of M_{b5}, pH, EC, major cation–anion concentrations of effluent, and their ratio to influent concentration (C_{out}/C_{in}) are shown as a function of PVF in Fig. 3a-d. M_{b5} was permeated for more than 10 months with TAL, and no

Table 1
Summary of the hydraulic conductivity of GCLs.

GCL	Permeation Liquid	MPUA (kg/m^2)	Hydration method	Hydraulic conductivity (m/s)	Permeation time (days)	Pore volumes of flow
M_{b3}	DIW	3.07	Non-prehydrated	4.6×10^{-11}	118	8.8
M_{b4}	DIW	4.13		2.9×10^{-11}	165	5.1
M_{b5}	DIW	4.85		2.1×10^{-11}	191	6.1
M_{b3}	TAL	3.30	Non-prehydrated	2.6×10^{-6}	0.02	30
M_{b4}	TAL	4.10		7.6×10^{-7}	0.11	35
M_{b5}	TAL	4.96		4.1×10^{-11}	314	12
M_{b3FF}	TAL	3.00	Non-prehydrated	6.7×10^{-11}	280	39
M_{b4FF}	TAL	4.00		6.1×10^{-11}	251	35
M_{b5FF}	TAL	5.00		7.2×10^{-11}	233	15
M_{b3P}	TAL	3.20	Prehydrated	1.6×10^{-10}	279	36
M_{b4P}	TAL	4.30		4.8×10^{-11}	280	21

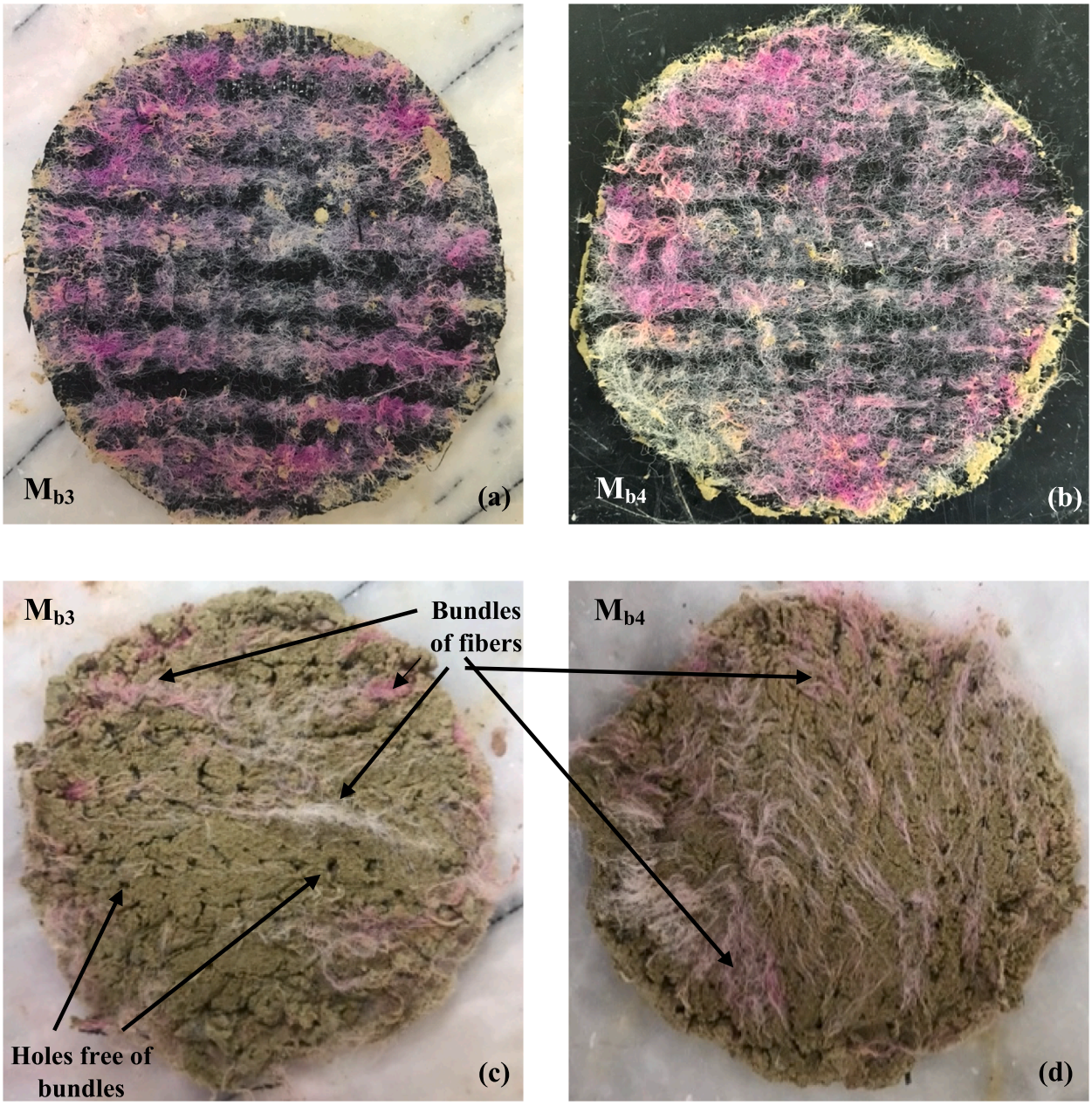

Fig. 2. Trace of preferential flow paths marked with pink color after dye test: a) M_{b3}, b) M_{b4}, c) M_{b3} without woven geotextile and d) M_{b4} without woven geotextile (woven geotextiles were removed from M_{b3} and M_{b4} after cutting the needle punched fibers with scalpel). (For interpretation of the references to color in this figure legend, the reader is referred to the web version of this article.)

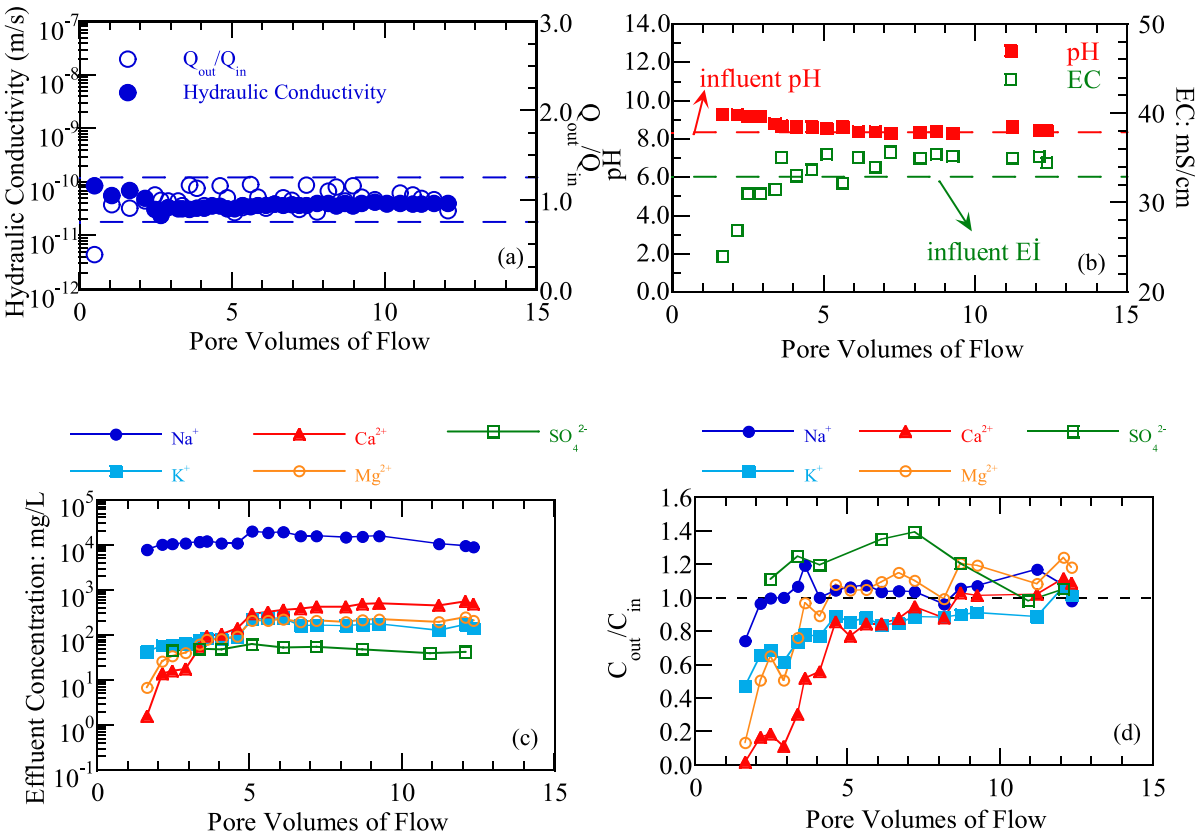

Fig. 3. Test results for M_{b5} permeated with TAL: a) Hydraulic conductivity, b) pH and EC of influent and effluent c) Na^+, K^+, Ca^{2+}, Mg^{2+}, and SO_4^{2-} concentrations in the effluent, d) effluent-to-influent ratio of Na^+, K^+, Ca^{2+}, Mg^{2+}, and SO_4^{2-}.

appreciable increase was observed in the hydraulic conductivity until the end of testing (Fig. 3a). The final hydraulic conductivity of M_{b5} to TAL was 4.1×10^{-11} m/s, which is significantly lower than that of M_{b3} and M_{b4}.

The pH and EC values of effluent samples taken throughout the hydraulic conductivity test of M_{b5} are shown as a function of PVF in Fig. 3b. The pH and EC values of the influent solution are also shown with dashed lines. The pH values of the effluent solution slightly decreased from 10.0 to 8.0, whereas the EC values significantly increased from 23 to 34 mS/cm during permeation (Fig. 3b). These trends are typical in cases where the EC of the permeant liquid is higher than the initial EC of the soil pore water (i.e., $EC_{in} > EC_{soil}$), and the pH_{out}/pH_{in} is initially greater than unity (i.e., $pH_{out}/pH_{in} > 1$) but slightly toward unity (Shackelford et al., 1999). The effluent pH and EC values were within ± 10 % of the influent, indicating that pH and EC equilibrium was achieved during testing of M_{b5}.

Fig. 3c shows the concentrations of major exchangeable cations (Na^+, K^+, Ca^{2+}, Mg^{2+}) and anion (SO_4^{2-}) detected in the effluents of M_{b5}. K^+, Ca^{2+}, Mg^{2+} and SO_4^{2-} slightly increased as the PVF increased. Since the most abundant cation species in TAL is Na^+ and GCL also includes an appreciable amount of Na^+, Na^+ concentration measured in the effluent was close to that of the influent (i.e. 14875 mg/L). To better represent the cation exchange in terms of breakthrough curves (Fig. 3d), the cation and anion concentrations in the effluent were divided into concentrations in the influent (C_{out}/C_{in}). The steady state condition was obtained at 3.0 PVF for Na^+ and at later PVF (i.e. 5.0 PVF) for K^+, Ca^{2+}, $Mg^{2+}$and SO_4^{2-}. Tian et al. (2017) showed that the hydraulic conductivity of Na-GCLs was not affected by the anion species present in the permeant, whereas the permeability of polymer-treated GCLs depended on the anion species. Note that there was no significant influence of SO_4^{2-} anions on the hydraulic conductivity of M_{b5} to TAL in this study.

To show the influence of MPUA on hydraulic conductivity, the final hydraulic conductivity of GCL permeated with TAL (K_{TAL}) was normalized with that of GCL to DIW (K_{DIW}). The hydraulic conductivity ratio of GCLs (K_{TAL} / K_{DIW}) is plotted as a function of MPUA and is shown in Fig. 4. Fig. 4 shows that the hydraulic performances of M_{b3} and M_{b4} were significantly affected by TAL. In contrast, increasing the MPUA to 5.0 kg/m^2 decreased the hydraulic conductivity, which resulted in a hydraulic conductivity ratio around unity (K_{TAL} / $K_{DIW} \approx 1$).

Chen et al. (2018) reported the hydraulic conductivity of Na-GCL to TAL. Two Na-GCLs with different bentonite granule sizes (CS and GS) were used, and the MPUA of the GCL was 3.76 ± 0.12 kg/m^2. These data are also plotted in Fig. 4 for comparison. K_{TAL} / K_{DIW} of CS-GCL was comparable with that of this study, whereas GS-GCL was ten times lower than K_{TAL} / K_{DIW} of CS-GCL, M_{b3}, and M_{b4} (Fig. 4). The difference between the CS and GS-GCLs can be attributed to the granule size of the bentonite. Because the granule size of GS bentonite was smaller than that of CS.

In another study, Chen et al. (2019) reported the influence of polymer loading on the hydraulic conductivity of bentonite polymer composite GCLs (BPC-GCLs) to CCPs leachates. In the case of TAL, the hydraulic conductivity of GCL with 1.2 % polymer loading (i.e. CP-1.2 GCL) was 6.8×10^{-7} m/s. The hydraulic conductivity decreased to 4.2×10^{-12} m/s when the polymer loading was increased to 5.1 %. Since the influence of polymer loading was negligible at 1.2 %, data regarding this value is also plotted in Fig. 4. As seen in Fig. 4, K_{TAL} / K_{DIW} of CP-1.2 GCL was also comparable with K_{TAL} / K_{DIW} in this study.

Chen et al., (2018, 2019) and the findings presented here show that MPUA is a critical parameter when the permeant solution is TAL. Because the hydraulic conductivity of GCLs was high (i.e., $> 1.0 \times 10^{-9}$ m/s) within the MPUA range of 3.0 and 4.0 kg/m^2 and low around 5.0 kg/m^2 ($\leq 1.0 \times 10^{-9}$ m/s). The existence of bundles of fibers plays an important role in governing the flow across the GCLs when the MPUA is less than 4.0 kg/m^2. Conversely, increasing the MPUA to 5.0 kg/m^2

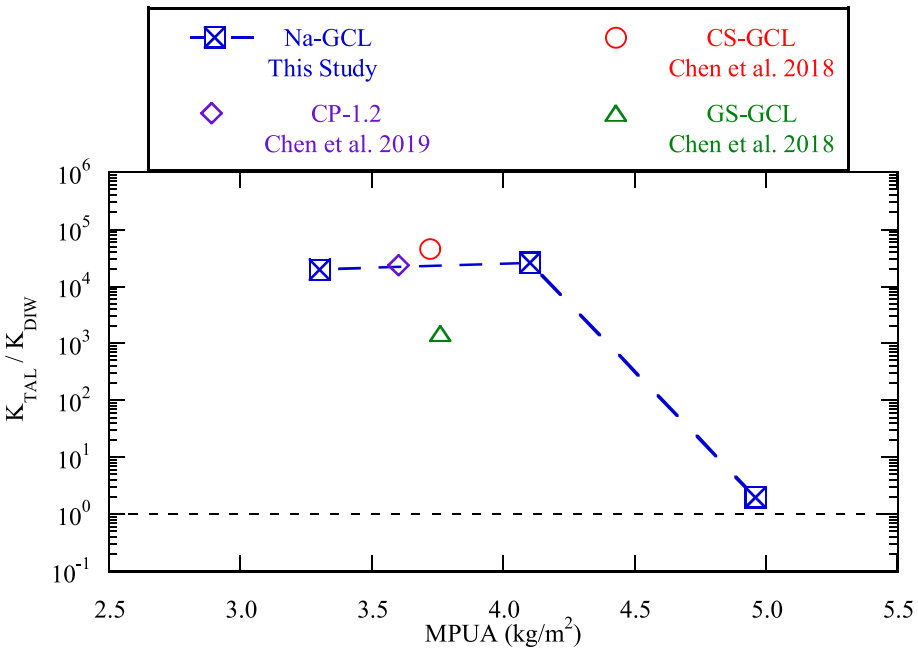

Fig. 4. Hydraulic conductivity to TAL relative to hydraulic conductivity to deionized water (K_{TAL} / K_{DIW}) as a function of mass per unit area (MPUA) of GCLs.

masks the role of bundles of fiber in hydraulic conductivity.

4.2. Post-Test evaluation of GCLs

The exchangeable bound cations in bentonite obtained after direct permeation with TAL are summarized in Table S3. Cation mole fractions (i.e. X_{Na}, X_K, X_{Ca}, X_{Mg}) were computed as the ratio of the associated cation concentration to the total concentration of the exchangeable major cations (i.e. Na^+, K^+, Ca^{2+} and Mg^{2+}). The change in the exchangeable cation mole fractions is evaluated as a function of MPUA and is shown in Fig. 5. The monovalent ($X_M = X_{Na} + X_K$) and divalent ($X_D = X_{Ca} + X_{Mg}$) cation mole fractions of virgin GCL were 79 % and 21 %, respectively. Depending on the MPUA of the GCL, monovalent cations in the GCL were replaced with divalent cations in the leachate (Fig. 5). Cation replacement was less pronounced in M_{b3}. The mole fractions of monovalent cations slightly decreased from 79 % to 78 % for M_{b3} and 75 % for M_{b4}. In addition, the divalent cation mole fractions increased slightly from 21 % to 22 % and 25 % for M_{b3} and M_{b4}, respectively (Fig. 5).

Two possible reasons can be asserted for the limited cation exchange obtained for M_{b3} and M_{b4}. The first reason may be the permeation durations applied during the hydraulic conductivity tests. Since MPUA was low and thus flow mainly occurred through the bundles of fibers (Fig. 2), the total permeation time applied for M_{b3} was less than 1 h and almost 3 h for M_{b4}. Thus, bentonite could not react with TAL to propagate and complete the cation exchange within a limited time. However, M_{b5} was permeated with TAL for more than 10 months because of low hydraulic conductivity. However, the cation exchange was still negligible for M_{b5}, where X_M decreased to 71 % and X_D increased to 29 % (Fig. 5). Thus, the duration of permeation does not appear to be a major factor controlling the cation exchange reaction. The other reason may be the abundance of Na^+ ions in TAL, which limits the cation exchange between GCL and TAL. In a typical cation exchange reaction of Na-GCL, Na^+ concentration decreases and Ca^{2+} concentration increases in the effluent over time (Bradshaw et al., 2016; Bradshaw and Benson, 2013; Jo et al., 2005; Lee and Shackelford, 2005; Ören et al., 2020). However, in this study, although Ca^{2+} and Mg^{2+} concentrations increased, Na^+ concentration in the effluent did not significantly change with time (Fig. 3c). This shows that TAL was a potential source of Na^+ ions for GCLs throughout the test duration. Thus, the abundance of Na^+ in TAL appears to be the major factor accounting for the high mole fractions of Na^+ ions in GCLs.

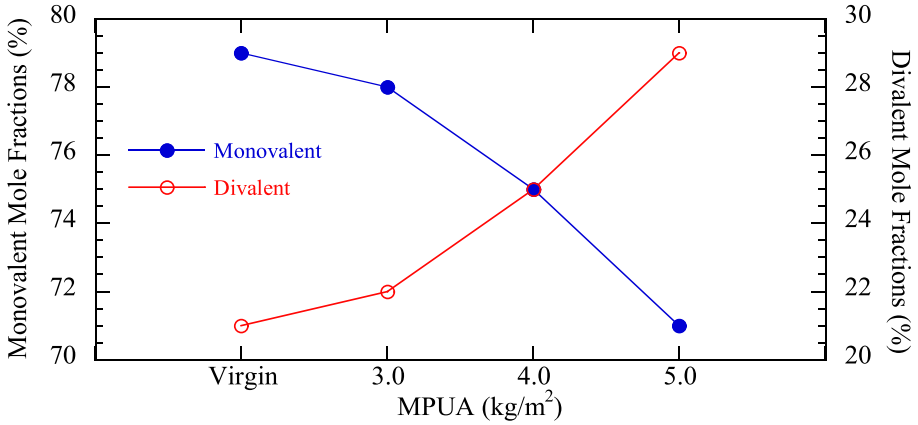

Fig. 5. Mole fractions of GCLs as a function of mass per unit area (MPUA).

The hydraulic conductivity of GCLs is strongly related to the swell index of bentonite (Jo et al., 2001; Kolstad et al., 2004). In other words, the main mechanism controlling the hydraulic conductivity of GCLs is the swelling of bentonite. To determine the swelling performance of the post-test GCLs, bentonite was removed from the GCLs and subjected to swell index tests with DIW. The post-test swell indices are shown in Fig. S3 as a function of MPUA. The swell indices of bentonite in DIW and TAL are also shown with dashed lines in Fig. S3. The swell index of bentonite in DIW was 22.5 mL/2g and that in TAL was 8.5 mL/2g. The swell indices of post-test M_{b3}, M_{b4}, and M_{b5} were 17.5, 16.8, and 15.8 mL/2g, respectively (Fig. S3). These values are closer to the swell index of bentonite in DIW than in TAL, indicating the high swelling potential of bentonite even after hydraulic conductivity tests. The reason why post-test swell indices were close to the swell index in DIW can be attributed to the abundance of Na^+ ions present in the exchangeable cation sites of bentonites. Indeed, the mole fraction of Na^+ in M_{b3}, M_{b4} and M_{b5} was ranged between 67 % and 72 % (Table S3). The hydrated ionic radius of Na^+ is larger than that of divalent and trivalent cations, resulting in a high thickness of the adsorbed water layer surrounding the bentonite (Bohn et al., 2001). The larger the thickness of the water layer, the higher the swell index.

As previously mentioned, the permeation duration was not a major factor controlling the cation exchange between GCL and TAL. However, it has a slight influence on the swell index of post-test bentonite. The swell indices of M_{b3}, M_{b4} and M_{b5} was expected to be the same within each other because these GCLs contain the same bentonite. However, the swell index slightly decreased from 17.5 to 15.8 mL/2g as MPUA increased from 3.0 to 5.0 kg/m^2 (Fig. S3). That is, the lowest swell index was obtained for the GCL, which had the lowest X_M and highest X_D (i.e. M_{b5}) (Fig. 5). The permeation duration was 10 months for M_{b5}, which means that the interaction between bentonite and TAL was quite long with respect to M_{b3} and M_{b4}, leading to the lowest swell index value for this GCL.

4.3. *Influence of bundles of fiber existence on hydraulic conductivity*

In terms of barrier performance, several studies have indicated that the hydraulic conductivity of GCLs can be affected by the bundles of fibers existing on GCLs (Rowe et al., 2017; Rowe and Hamdan, 2021). The osmotic swelling of bentonite decreases because of the cation exchange reaction that occurs between GCL and the leachate during permeation. Hence, the pressure exerted on the bundles of fibers decreases and preferential flow paths occur across the bundles, resulting in high hydraulic conductivity for the GCL (Rowe et al., 2019, 2017; Rowe and Hamdan, 2021; Scalia and Benson, 2011). Visual inspection of M_{b3} and M_{b4} after dye tests revealed that the flow mainly occurred through the needle-punched fiber bundles (Fig. 2). To identify the potential effect of bundles of fiber on hydraulic conductivity, additional tests were conducted on fiber-free GCLs with varying MPUAs (i.e. M_{b3FF}, M_{b4FF} and M_{b5FF}).

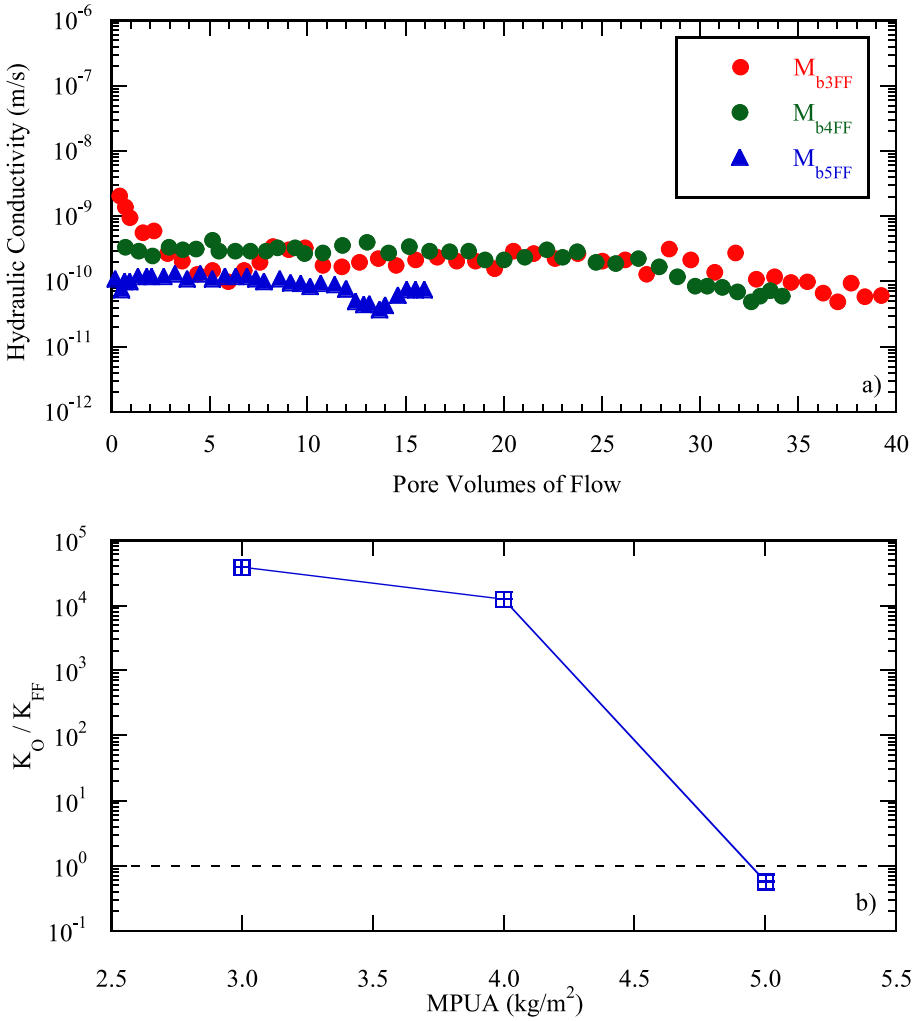

Fig. 6. A) hydraulic conductivity of fiber free gcls withmass per unit area (MPUA) of 3.0 kg/m^2 (M_{b3FF}), MPUA of 4.0 kg/m^2 (M_{b4FF}) and MPUA of 5.0 kg/m^2 (M_{b5FF}) as a function of PVF and b) hydraulic conductivity of original GCL relative to fiber-free GCL (K_O / K_{FF}) to TAL as a function of mass per unit area (MPUA) of GCLs.

The hydraulic conductivity behavior of fiber-free GCLs (M_{b3FF}, M_{b4FF}, M_{b5FF}) are shown in Fig. 6a. Regardless of MPUA, the hydraulic conductivity of the GCLs slightly decreased throughout the test duration. The final hydraulic conductivity was calculated as 6.7×10^{-11} m/s for M_{b3FF}, 6.1×10^{-11} m/s for M_{b4FF} and 7.2×10^{-11} for M_{b5FF} (Table 1).

The hydraulic conductivity of the original and fiber-free GCLs was compared in terms of the hydraulic conductivity ratio (K_O / K_{FF}). Fig. 6b shows K_O / K_{FF} of GCLs as a function of MPUA. The tests conducted on fiber-free GCLs proved the influence of bundles of fibers on the hydraulic conductivity of GCLs. The hydraulic conductivity of M_{b3} and M_{b4} was several orders of magnitude greater than those of M_{b3FF} and M_{b4FF} (Fig. 6b). The K_O / K_{FF} was 38,806 and 12,460 when MPUA was 3.0 and 4.0 kg/m^2, respectively. Bentonite granules started to close the flow paths within the bundles of fibers by increasing the MPUA from 3.0 to 4.0 kg/m^2, indicating a decrease in the hydraulic conductivity by a factor of 3.0. Increasing the MPUA to 5.0 kg/m^2 decreased K_O / K_{FF} to approximately unity (Fig. 6b), which means that the existence of bundles of fibers on GCLs may not pose a risk in terms of hydraulic conductivity when TAL is the permeant.

To compare with M_{b5}, effluent and influent concentrations, pH, and EC measurements were determined only for M_{b5FF}. The hydraulic behavior of M_{b5FF} was similar to that of M_{b5} (Fig. S4a), where the final hydraulic conductivity of M_{b5FF} was 7.2×10^{-11} m/s (Table 1). Although the change in pH of the effluent over time for M_{b5FF} resembles that of M_{b5}, the behavioral change in the EC of effluent between M_{b5FF} and M_{b5} was rather different (Fig. S4b). However, pH_{out}/pH_{in} and EC_{out}/EC_{in} were close to 1.0 (or around unity) at the time of termination in both tests. The Na^+ concentrations detected in the effluents of M_{b5FF} slightly decreased to 10^4 mg/L during the test, which was close to that of M_{b5}. The concentrations of other cations (K^+, Ca^{2+} and Mg^{2+}) present in the effluents were similar for both M_{b5FF} and M_{b5} (Fig. S4c). C_{out}/C_{in} ratios of the anion and cations were around unity, indicating that chemical equilibrium was established for M_{b5FF} as well (Fig. S4d).

4.4. Influence of prehydration on hydraulic conductivity

Some researchers have pointed out that the order of the permeant liquids introduced into the GCL has a substantial impact on hydraulic conductivity (Chen et al., 2018; Di Emidio et al., 2015; Petrov et al., 1997; Petrov and Rowe, 1997; Shackelford et al., 2000). In particular,

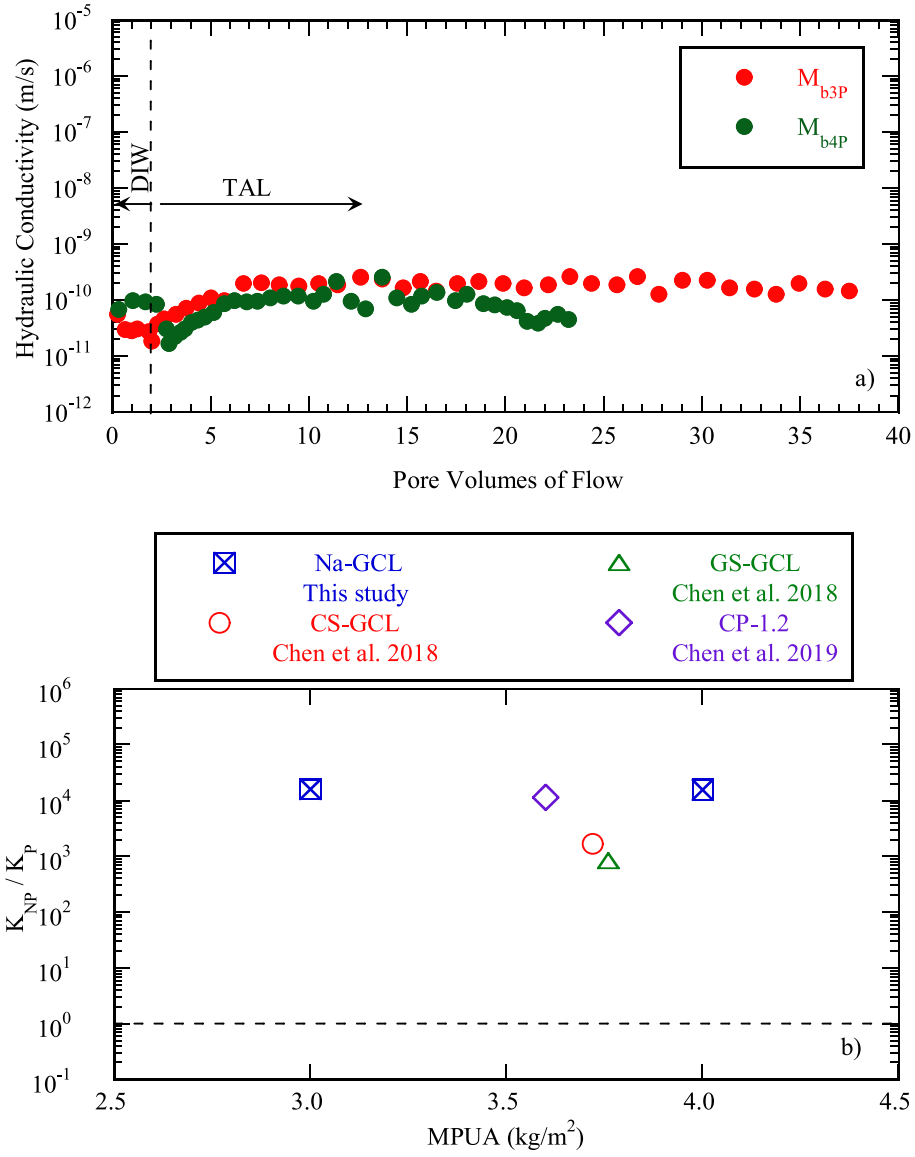

Fig. 7. A) hydraulic conductivity of prehydrated gcls withmass per unit area (MPUA) of 3.0 kg/m^2 (M_{b3P}) and MPUA of 4.0 kg/m^2 (M_{b4P}) and b) hydraulic conductivity of non-prehydrated GCL relative to prehydrated GCL (K_{NP} / K_P) to TAL as a function of mass per unit area (MPUA) of GCLs.

hydrating the bentonite with DIW before permeation with a chemical solution generally results in lower hydraulic conductivity than direct permeation (first exposure effect) (Bouazza, 2002; Mazzieri et al., 2000; Ruhl and Daniel, 1997; Shackelford et al., 2000).

The influence of prehydration on the hydraulic conductivity of GCLs has scarcely been investigated as a function of MPUA. Therefore, additional tests were conducted to determine whether prehydration influences hydraulic conductivity of M_{b3} and M_{b4}. These two GCLs were selected because they had high hydraulic conductivity to TAL ($>1.0 \times 10^{-9}$ m/s) (Fig. 1). For this purpose, the GCLs were initially permeated with DIW until 2.0 PVF before permeating with TAL. The hydraulic conductivity of both GCLs to DIW was comparable with the hydraulic conductivity of GCLs to DIW given in Table 1. After the prehydration stage was completed, the permeant solution was switched to the TAL solution, and the hydraulic conductivity of the GCLs (i.e. M_{b3P} and M_{b4P}) was measured (Fig. 7a). The hydraulic conductivity slightly increased during permeation with TAL and finally reached to 1.6×10^{-10} m/s and 4.8×10^{-11} m/s for M_{b3P} and M_{b4P}, respectively (Table 1), indicating an improvement in the barrier performance of M_{b3} and M_{b4} with prehydration.

The influence of prehydration on the hydraulic performance of GCLs is shown in Fig. 7b in terms of the hydraulic conductivity ratio (K_{NP} / K_P). K_{NP} / K_P refers to the ratio of the hydraulic conductivity of non-prehydrated GCLs to that of prehydrated GCLs. Some data taken from the literature are also shown in Fig. 7b for comparison. The hydraulic conductivity of non-prehydrated GCLs (i.e. M_{b3} and M_{b4}) was four orders of magnitude greater than that of prehydrated GCLs (i.e. M_{b3P} and M_{b4P}) (Fig. 7b), which is also in agreement with the literature (Chen et al., 2019; Chen et al., 2018). GCLs prehydrated with DIW allow bentonite to exhibit osmotic swelling, providing less pore space available between the particles for mobile water (Athanassopoulos et al., 2015; Benson et al., 2018a; Katsumi et al., 2007; Wang et al., 2019). Hence, the flow across the GCLs was still low when the permeating liquid was switched to TAL.

5. Summary and conclusions

In this study, the hydraulic conductivity of Na-GCL to TAL was investigated and discussed in terms of MPUA, bundles of fiber existence, and prehydration conditions. For this purpose, original and fiber-free GCLs with MPUAs of 3.0 kg/m^2, 4.0 kg/m^2 and 5.0 kg/m^2 were subjected to hydraulic conductivity tests.

The influence of MPUA was negligible when the permeant was DIW. However, the impact of MPUA was significant when GCLs were directly permeated with TAL. The hydraulic conductivity of M_{b3} and M_{b4} was high (2.6×10^{-6} and 7.6×10^{-7} m/s, respectively), whereas the hydraulic conductivity of M_{b5} was 4.1×10^{-11} m/s, which was comparable with the hydraulic conductivity of M_{b5} to DIW. Dye tests performed on M_{b3} and M_{b4} after hydraulic conductivity tests showed that flow preferentially occurred through the bundles of fibers existing in M_{b3} and M_{b4}. The amount of bentonite was not sufficient in M_{b3} and M_{b4} to supply adequate confining stress on the bundles. Thus, the bundles functioned as capillary tubes that wick the permeant solution.

Chemical analyses conducted on influent and effluent solutions and on bentonite showed that negligible cation replacement occurred between GCLs and TAL solutions. Although Na^+ ions in bentonite were replaced with divalent cations present in TAL (e.g. Ca^{2+}), the vacant sites in exchangeable cation sites were filled with Na^+ ions again, which were supplied by TAL.

The post-test swell index of GCLs was found to be within the range of 15.8 – 17.5 mL/2g, which was lower than that in DIW 22.5 mL/2g and greater than that in TAL (8.5 mL/2g). Thus, rather than cation exchange, MPUA and the existence of bundles of fibers governed the hydraulic conductivity of GCLs to TAL.

To quantify the influence of bundles of fibers on the hydraulic conductivity, M_{b3}, M_{b4} and M_{b5} were prepared in fiber-free conditions using the same bentonite (M_{b3FF}, M_{b4FF} and M_{b5FF} respectively) and subjected to hydraulic conductivity tests with TAL. The hydraulic conductivities of M_{b3FF} and M_{b4FF} were almost four orders of magnitude lower than those of M_{b3} and M_{b4}, whereas M_{b5FF} was close to M_{b5}, indicating the role of bundles of fibers in the hydraulic conductivity of GCL.

To observe the influence of prehydration on M_{b3} and M_{b4}, these GCLs were permeated with DIW for approximately two PVF, and then the permeation was switched to TAL. The hydraulic conductivities of prehydrated M_{b3P} and M_{b4P} were 1.6×10^{-10} m/s and 4.8×10^{-11} m/s, respectively, and were considerably lower than those of non-prehydrated GCLs.

Declaration of competing interest

The authors declare the following financial interests/personal relationships which may be considered as potential competing interests: A. Hakan Oren reports financial support was provided by Scientific and Technological Research Council of Turkey.

Data availability

Data will be made available on request.

Acknowledgement

This study was financially supported by The Scientific and Technological Research Council of Türkiye (TÜBİTAK) with Grant No: 119R044. The authors are grateful to TÜBİTAK for their valuable support.

Appendix A. Supplementary data

Supplementary data to this article can be found online at https://doi.org/10.1016/j.wasman.2023.11.033.

References

Akin, I.D., Chen, J., Likos, W.J., Benson, C.H., 2017. Water Vapor Sorption of Bentonite-Polymer Mixtures Contacted with Aggressive Leachates 209–218. https://doi.org/10.1061/9780784480434.021.

ASTM D4318-17, 2017. Standard Test Methods for Liquid Limit, Plastic Limit, and Plasticity Index of Soils, in: ASTM International, West Conshohocken, PA, USA. pp. 1–14. https://doi.org/10.1520/D4318.

ASTM D5890-19, 2019. Standard Test Method for Swell Index of Clay Mineral Component of Geosynthetic, in: Annual Book of ASTM Standards. pp. 20–23. https://doi.org/10.1520/D5890-19.2.

Astm d5993–99,, 2010. Standard Test Method for Measuring Mass Per Unit of Geosynthetic Clay Liners. ASTM Int. West Conshohocken, PA, USA 99, 1–4. https://doi.org/10.1520/D5993-99R09.2.

ASTM:D6766-14, 2014. Standard Test Method for Evaluation of Hydraulic Properties of Geosynthetic Clay. ASTM Int. West Conshohocken, PA, USA i, 1–9. https://doi.org/10.1520/D6766-18.2.

ASTM:D7503-18, 2020. Standard Test Method for Measuring the Exchange Complex and Cation Exchange Capacity of Inorganic Fine-Grained Soils 1. ASTM Int. West Conshohocken, PA, USA 1–5. https://doi.org/10.1520/D7503.

Athanassopoulos, C., Benson, C., Donovan, M., Chen, J., 2015. Hydraulic Conductivity of a Polymer - Modified GCL Permeated with High - pH Solutions. Geosynth. 2015, 181–186.

Benson, C.H., Ören, A.H., Gates, W.P., 2010. Hydraulic conductivity of two geosynthetic clay liners permeated with a hyperalkaline solution. Geotext. Geomembranes 28, 206–218. https://doi.org/10.1016/j.geotexmem.2009.10.002.

Benson, C.H., Chen, J.N., Edil, T.B., Likos, W.J., 2018a. Hydraulic Conductivity of Compacted Soil Liners Permeated with Coal Combustion Product Leachates. J. Geotech. Geoenvironmental Eng. 144, 04018011. https://doi.org/10.1061/(asce)gt.1943-5606.0001855.

Benson, C.H., Chen, J.N., Edil, T.B., Likos, W.J., 2018b. Hydraulic conductivity of compacted soil liners permeated with coal combustion product leachates. J. Geotech. Geoenvironmental Eng. 144, 1–15. https://doi.org/10.1061/(ASCE)GT.1943-5606.0001855.

Bohn, H.L., McNeal, B.L., O'Connor, G.A., 2001. Soil chemistry. Wiley.

Bradshaw, S.L., Benson, C.H., Scalia, J., 2013. Hydration and cation exchange during subgrade hydration and effect on hydraulic conductivity of geosynthetic clay liners. J. Geotech. Geoenvironmental Eng. 139, 526–538. https://doi.org/10.1061/(ASCE)GT.1943-5606.0000793.

Chen, J.N., Benson, C.H., Edil, T.B., 2018. Hydraulic Conductivity of Geosynthetic Clay Liners with Sodium Bentonite to Coal Combustion Product Leachates. J. Geotech. Geoenvironmental Eng. 144, 04018008. https://doi.org/10.1061/(ASCE)GT.1943-5606.0001844.

Chen, J., Salihoglu, H., Benson, C.H., Likos, W.J., Edil, T.B., 2019. Hydraulic Conductivity of Bentonite-Polymer Composite Geosynthetic Clay Liners Permeated with Coal Combustion Product Leachates. J. Geotech. Geoenvironmental Eng. 145, 04019038. https://doi.org/10.1061/(asce)gt.1943-5606.0002105.

Demir Sürer, A.İ., 2023. Hydraulic conductivity of geosynthetic clay liners (GCLs) to coal combustion and trona ash leachates, M.Sc. Thesis, Dokuz Eylul University, Graduate School of Natural and Applied Sciences, 1-96.

Di Emidio, G., Mazzieri, F., Verástegui-Flores, R.-D., Van Impe, W., Bezuijen, A., 2015. Polymer-treated bentonite clay for chemical-resistant geosynthetic clay liners. Geosynth. Int. 22, 1–13. https://doi.org/10.1680/gein.14.00036.

Fox, P.J., Triplett, E.J., Kim, R.H., Olsta, J.T., 1998. Field Study of Installation Damage for Geosynthetic Clay Liners. Geosynth. Int. 5, 491–520.

Guyonnet, D., Touze-Foltz, N., Norotte, V., Pothier, C., Didier, G., Gailhanou, H., Blanc, P., Warmont, F., 2009. Performance-based indicators for controlling geosynthetic clay liners in landfill applications. Geotext. Geomembranes 27, 321–331. https://doi.org/10.1016/j.geotexmem.2009.02.002.

Jo, H.Y., Katsumi, T., Benson, C.H., Edil, T.B., 2001. Hydraulic conductivity and swelling of nonprehydrated GCLs permeated with single-species salt solutions. J. Geotech. Geoenvironmental Eng. 127 (7), 557–567.

Jo, H.Y., Benson, C.H., Edil, T.B., 2004. Hydraulic conductivity and cation exchange in non-prehydrated and prehydrated bentonite permeated with weak inorganic salt solutions. Clays Clay Miner. 52, 661–679.

Jo, H.Y., Benson, C.H., Shackelford, C.D., Lee, J.-M., Edil, T.B., 2005. Long-term hydraulic conductivity of a geosynthetic clay liner permeated with inorganic salt solutions. J. Geotech. Geoenvironmental Eng. 131, 405–417. https://doi.org/10.1061/(ASCE)1090-0241(2005)131:4(405).

Jones, K.B., Ruppert, L.F., Swanson, S.M., 2012. Leaching of elements from bottom ash, economizer fly ash, and fly ash from two coal-fired power plants. Int. J. Coal Geol. 94, 337–348. https://doi.org/10.1016/j.coal.2011.10.007.

Katsumi, T., Ishimori, H., Ogawa, A., Yoshikawa, K., Hanamoto, K., Fukagawa, R., 2007. Hydraulic Conductivity of Nonprehydrated Geosynthetic Clay Liners Permeated With Inorganic Solutions and Waste Leachates. Soils Found. 47, 79–96. https://doi.org/10.3208/sandf.47.79.

Katsumi, T., Ishimori, H., Onikata, M., Fukagawa, R., 2008. Long-term barrier performance of modified bentonite materials against sodium and calcium permeant solutions. Geotext. Geomembranes 26, 14–30. https://doi.org/10.1016/j.geotexmem.2007.04.003.

Kolstad, D., Benson, C., Edil, T., 2004. Hydraulic conductivity and swell of nonprehydrated geosynthetic clay liners permeated with multispecies inorganic solutions. J. Geotech. 1236–1249 https://doi.org/10.1061/(ASCE)1090-0241(2004)130.

Lee, J.-M., Shackelford, C.D., 2005. Concentration dependency of the prehydration effect for a geosynthetic clay liner. Soils Found. 45, 27–41.

Liu, Y., Bouazza, A., Gates, W.P.P., Rowe, R.K.K., 2015. Hydraulic performance of geosynthetic clay liners to sulfuric acid solutions. Geotext. Geomembranes 43, 14–23. https://doi.org/10.1016/j.geotexmem.2014.11.004.

Mazzieri, F., Emidio, G.D., 2015. Hydraulic conductivity of a dense prehydrated geosynthetic clay liner. Geosynth. Int. 22, 138–148.

Mazzieri, F., Di Emidio, G., Fratalocchi, E., Di Sante, M., Pasqualini, E., 2013. Permeation of two GCLs with an acidic metal-rich synthetic leachate. Geotext. Geomembranes 40, 1–11. https://doi.org/10.1016/j.geotexmem.2013.07.011.

Naka, A., Flores, G., Inui, T., Sakanakura, H., Katsumi, T., 2019. Hydraulic performance and chemical compatibility of a powdered Na-bentonite geosynthetic clay liner permeated with mine drainage. Soils Found. 59, 1128–1147. https://doi.org/10.1016/j.sandf.2019.02.005.

Ören, A.H., Akar, R.Ç., 2017. Swelling and hydraulic conductivity of bentonites permeated with landfill leachates. Appl. Clay Sci. 142, 81–89. https://doi.org/10.1016/j.clay.2016.09.029.

Ören, A.H., Öztürk, M., Kul, T.Ö., Nart, Z., 2018. Barrier performance of geosynthetic clay liners to copper (II) chloride solutions. Environ. Geotech. 7, 491–500. https://doi.org/10.1680/jenge.18.00024.

Ören, A.H., Taşkesti, B.E., Özdamar, T., 2022. Evaluating the Hydration and Hydraulic Performance of a Geosynthetic Clay Liner (GCL) in Terms of Bentonite Mass per Unit Area. Int. J. Geosynth. Gr. Eng. 4 https://doi.org/10.1007/s40891-022-00372-4.

Petrov, R.J., Rowe, R.K., Quigley, R., 1997. Selected factors influencing GCL hydraulic conductivity. J. Geotech. Geoenvironmental Eng. 123, 683–695.

Polat, F., 2022. Investigating the barrier performance of geosynthetic clay liners (GCLs) to calcium chloride solutions in terms of mass per unit area of bentonite and needle punching density, M.Sc. Thesis, Dokuz Eylul University, Graduate School of Natural and Applied Sciences, 1-85.

Rowe, R.K., Brachman, R.W.I., Hosney, M.S., Take, W.A., Arnepalli, D.N., 2017. Insight into hydraulic conductivity testing of geosynthetic clay liners (GCLs) exhumed after 5 and 7 years in a cover. Can. Geotech. J. 1138, 1118–1138.

Rowe, R.K., Hamdan, S., 2021a. Effect of wet-dry cycles on standard & polymer-amended GCLs in covers subjected to flow over the GCL. Geotext. Geomembranes 49, 1165–1175. https://doi.org/10.1016/j.geotexmem.2021.03.010.

Rowe, R.K., Hamdan, S., 2021b. Effect of wet-dry cycles on standard & polymer-amended GCLs in covers subjected to flow over the GCL. Geotext. Geomembranes 49. https://doi.org/10.1016/j.geotexmem.2021.03.010.

Ruhl, L., Vengosh, A., Dwyer, G.S., Hsu-Kim, H., Schwartz, G., Romanski, A., Smith, S.D., 2012. The impact of coal combustion residue effluent on water resources: A north carolina example. Environ. Sci. Technol. 46, 12226–12233. https://doi.org/10.1021/es303263x.

Salemi, N., Abtahi, S.M., Rowshanzamir, M., Hejazi, S.M., 2018. Geosynthetic clay liners: effect of structural properties and additives on hydraulic performance and durability. Environ. Earth Sci. 77, 1–13. https://doi.org/10.1007/s12665-018-7364-z.

Scalia, J., Benson, C.H., Bohnhoff, G.L., Edil, T.B., Shackelford, C.D., 2014. Long-term hydraulic conductivity of a bentonite-polymer composite permeated with aggressive inorganic solutions. J. Geotech. Geoenvironmental Eng. 140, 1–13. https://doi.org/10.1061/(ASCE)GT.1943-5606.0001040.

Setz, M.C., Tian, K., Benson, C.H., Bradshaw, S.L., 2017. Effect of ammonium on the hydraulic conductivity of geosynthetic clay liners. Geotext. Geomembranes 45, 665–673. https://doi.org/10.1016/j.geotexmem.2017.08.008.

Shackelford, C.D., Sample-Lord, K.M., 2014. Hydraulic conductivity and compatibility of bentonite for hydraulic containment barriers. Geo-Congress 2014 Febr. 23-26, 2014 | Atlanta, Georg. 370–387. https://doi.org/10.1061/9780784413265.030.

Shackelford, C.D., Benson, C.H., Katsumi, T., Edil, T.B., Lin, L., 2000. Evaluating the hydraulic conductivity of GCLs permeated with non-standard liquids. Geotext. Geomembranes 18, 133–161. https://doi.org/10.1016/S0266-1144(99)00024-2.

Sönmez, G., Işık, M., 2020. Kömür Yanma Atıklarının Çevresel Etkileri ve Kullanım Alanları. Ömer Halisdemir Üniversitesi Mühendislik Bilim. Derg. 9, 72–83. https://doi.org/10.28948/ngumuh.546144.

Stark, T.D., Akhtarshad, R., Choi, H., 2004. Occurrence and effect of bentonite migration in geosynthetic clay liners. Geosynth. Int. 11, 296–310. https://doi.org/10.1680/gein.2004.11.4.296.

Tan, Y., Basantis, A., Benson, C.H., Chen, J., 2022. Hydraulic Properties of Sluiced Coal Combustion Products Disposed in Impoundments, in: Geo-Congress 2022 GSP 335. pp. 505–513. https://doi.org/10.1061/9780784484050.052.

Von Maubeuge, K.P., Ehrenberg, H., 2014. Investigation of bentonite mass per unit area requirements for Geosynthetic Clay Liners. 10th Int. Conf. Geosynth. ICG 2014.

Wang, B., Xu, J., Chen, B., Dong, X., Dou, T., 2019. Hydraulic conductivity of geosynthetic clay liners to inorganic waste leachate. Appl. Clay Sci. 168, 244–248. https://doi.org/10.1016/j.clay.2018.11.021.

Wang, Y., Yu, J., Wang, Z., Liu, Y., Zhao, Y., 2021. A review on arsenic removal from coal combustion: Advances, challenges and opportunities. Chem. Eng. J. 414, 128785 https://doi.org/10.1016/j.cej.2021.128785.

Wireko, C., Abichou, T., Tian, K., Zainab, B., Zhang, Z., 2022. Effect of incineration ash leachates on the hydraulic conductivity of bentonite-polymer composite geosynthetic clay liners. Waste Manag. 139, 25–38. https://doi.org/10.1016/j.wasman.2021.12.011.

Yang, Y.-L., Reddy, K.R., Du, Y.-J., Fan, R.-D., 2018. Short-Term Hydraulic Conductivity and Consolidation Properties of Soil-Bentonite Backfills Exposed to CCR-Impacted Groundwater. J. Geotech. Geoenvironmental Eng. 144 https://doi.org/10.1061/(asce)gt.1943-5606.0001877.

Zainab, B., Tian, K., 2020. Geo-Congress 2020 GSP 316 289. pp. 579–586.

Zainab, B., Wireko, C., Li, D., Tian, K., Abichou, T., 2021. Hydraulic conductivity of bentonite-polymer geosynthetic clay liners to coal combustion product leachates. Geotext. Geomembranes 49, 1129–1138. https://doi.org/10.1016/j.geotexmem.2021.03.007.

Zhang, X., 2014. Management of coal combustion wastes, IEA Clean Coal Centre, Report number: CCC/231 ISBN 978-92-9029-551-8.